THE JOURNAL OF BIOLOGICAL CHEMISTRY
Vol. 272, No. 44, Issue of October 31, pp. 27919–27930, 1997

Printed in U.S.A.

Fidelity of *Escherichia coli* DNA Polymerase III Holoenzyme

THE EFFECTS OF β, γ COMPLEX PROCESSIVITY PROTEINS AND ε PROOFREADING EXONUCLEASE ON NUCLEOTIDE MISINCORPORATION EFFICIENCIES*

(Received for publication, March 19, 1997, and in revised form, July 28, 1997)

Linda B. Bloom‡§¶, Xiluo Chen‡§, D. Kuchnir Fygenson‡‖, Jennifer Turner, Mike O'Donnell**, and Myron F. Goodman‡ ‡‡**

*From the ‡Department of Biological Sciences, Hedco Molecular Biology Laboratories, University of Southern California, Los Angeles, California 90089-1340 and the **Microbiology Department, the Hearst Research Foundation, and the Howard Hughes Medical Institute, Cornell University Medical College, New York, New York 10021*

The fidelity of *Escherichia coli* DNA polymerase III (pol III) is measured and the effects of β, γ processivity and ε proofreading subunits are evaluated using a gel kinetic assay. Pol III holoenzyme synthesizes DNA with extremely high fidelity, misincorporating dTMP, dAMP, and dGMP opposite a template G target with efficiencies $f_{inc} = 5.6 \times 10^{-6}$, 4.2×10^{-7}, and 7×10^{-7}, respectively. Elevated dGMP·G and dTMP·G misincorporation efficiencies of 3.2×10^{-5} and 5.8×10^{-4}, attributed to a "dNTP-stabilized" DNA misalignment mechanism, occur when C and A, respectively, are located one base downstream from the template target G. At least 92% of misinserted nucleotides are excised by pol III holoenzyme in the absence of a next correct "rescue" nucleotide. As rescue dNTP concentrations are increased, pol III holoenzyme suffers a maximum 8-fold reduction in fidelity as proofreading of mispaired primer termini are reduced in competition with incorporation of a next correct nucleotide. Compared with pol III holoenzyme, the α holoenzyme, which cannot proofread, has 47-, 32-, and 13-fold higher misincorporation rates for dGMP·G, dTMP·G, and dAMP·G mispairs. Both the β, γ complex and the downstream nucleotide have little effect on the fidelity of catalytic α subunit. An analysis of the gel kinetic fidelity assay when multiple polymerase-DNA encounters occur is presented in the "Appendix" (see Fygenson, D. K., and Goodman, M. F. (1997) *J. Biol. Chem.* 272, 27931–27935 (accompanying paper)).

The first *in vitro* measurement of DNA synthesis fidelity was carried out by Kornberg and co-workers in 1962 (1) to analyze the mutagenic behavior of 5-bromouracil. Pol I[1] was found to misincorporate dGMP more readily opposite template bromouracil than opposite T, thus providing a biochemical basis for understanding bromouracil's ability to stimulate A·T → G·C transition mutations in *Escherichia coli* and bacteriophage T4 (2, 3). The next 3 decades bore witness to a wide range of fidelity studies investigating the biochemical basis of spontaneous and base analog-induced mutagenesis. These studies focused primarily on elucidating the properties of DNA polymerases and proofreading 3′-exonucleases and on developing and implementing methods to measure *in vitro* and *in vivo* mutational spectra. A comprehensive review of the first 30 years of fidelity studies is contained in Refs. 4 and 5.

DNA polymerases by themselves synthesize DNA with relatively low processivity. However, polymerases can interact with groups of accessory proteins to carry out processive chromosomal replication. The first experiments to identify and characterize proteins that confer high processivity were performed by Alberts, Nossal, and co-workers (6, 7) using T4 bacteriophage. These studies were instrumental for the subsequent development of *in vitro* systems to study replication holoenzymes from *E. coli* (8–10), T7 bacteriophage (11), and eucaryotes (12, 13).

E. coli β subunit is required to allow pol III core to attain high processivity (8, 14). X-ray diffraction data show that the β subunit is a doughnut-shaped dimer that can form a ring around DNA (15) and functions as a sliding clamp that inhibits dissociation of pol III core from DNA during chain elongation (14). The five-subunit γ complex is required to load β onto DNA (9, 10). The processivity of pol III core alone is only 10–20 nucleotides (16), while in the presence of β and γ complex it is increased to greater than 5000 nucleotides (8, 14).

Analysis of the specific effects of β, γ complex on fidelity is key to understanding the effect of processivity proteins on base substitution and frameshift mutations. It has been shown that mutations in T4 polymerase accessory proteins *in vivo* can cause both mutator and antimutator effects on the levels of spontaneous base substitution mutations (17). A measurement of T7 pol fidelity in an *in vitro* gap-filling assay suggests that processive synthesis, requiring the presence of thioredoxin, leads to an elevation in base substitutions and simple frameshift mutations in nonrepetitive sequences (18). A recent study

* This work was supported by National Institutes of Health Grants GM21422 and GM42554 (to D. K. F.) and by a grant from The Jane Coffin Childs Memorial Fund for Medical Research. The costs of publication of this article were defrayed in part by the payment of page charges. This article must therefore be hereby marked "*advertisement*" in accordance with 18 U.S.C. Section 1734 solely to indicate this fact.

§ The first and second authors contributed equally to this work.

¶ Present address: Dept. of Chemistry and Biochemistry, Arizona State University, Tempe, AZ 85287-1604.

‖ Fellow of The Jane Coffin Childs Memorial Fund for Medical Research.

‡‡ To whom correspondence should be addressed: Dept. of Biological Sciences, University of Southern California, SHS Rm. 172, University Park, Los Angeles, CA 90089-1340. Tel.: 213-740-5190; Fax: 213-740-8631; E-mail: mgoodman@mizar.usc.edu.

[1] The abbreviations used are: pol I, *E. coli* DNA polymerase I; pol III, *E. coli* DNA polymerase III; pol III core, comprised of α (polymerase), ε (3′ → 5′ proofreading exonuclease), and θ; pol III holoenzyme, comprised of pol III core + β (sliding processivity clamp) + γ complex (clamp loading complex containing γ, γ′, δ, χ, ψ); α holoenzyme, comprised of α + β, γ complex; pol δ; eucaryotic DNA polymerase δ; p/t, primer/template; SSB, *E. coli* single-stranded DNA-binding protein; **T** (in boldface), refers to the template target site at which fidelity is measured and should not be confused with T which refers to a template thymine; SCH, single completed hit conditions referring to extension of a primer via interaction with a DNA polymerase at most once, followed by polymerase dissociation; MCH, multiple completed hit conditions referring to extension of a primer via multiple interactions with DNA polymerase.

of eucaryotic pol δ suggests that nucleotide misincorporation efficiencies are increased in the presence of the proliferating cell nuclear antigen sliding clamp, a eucaryotic sliding clamp analogous to the *E. coli* β subunit (19).

In this paper, we analyze the individual and combined effects of the β, γ complex and ε proofreading exonuclease on nucleotide misincorporation efficiencies using a generalized gel kinetic assay (20). We compare fidelities at the same p/t DNA site for α subunit, α holoenzyme, pol III core, and pol III holoenzyme; α is the polymerase subunit of pol III core, which lacks proofreading activity. We also quantify a fundamental hallmark of proofreading, the dependence of pol III holoenzyme fidelity on the concentration of next correct dNTP.

Fidelity measurements for enzymes with poor processivity and/or high fidelity, such as are reported here, require pushing the limits of the gel kinetic assay. In the "Appendix" (see accompanying paper (60)), we provide an analysis that extends the usefulness of the assay by allowing for multiple encounters between DNA polymerase and DNA. This important generalization facilitates measurements of high fidelities with or without proofreading or processivity proteins.

EXPERIMENTAL PROCEDURES

Materials

Enzymes—E. coli DNA pol III proteins were purified as described: α, ε, and γ (21); β (15); δ and δ′ (22); χ and ψ (23); and θ (24). Subassemblies of γ complex and core were constituted as described (24, 25). Enzyme reaction buffer contained 20 mM Tris-HCl, pH 7.5, 40 μg/ml bovine serum albumin, 5 mM dithiothreitol, 50 mM NaCl, and 8 mM $MgCl_2$. T4 polynucleotide kinase was purchased from U. S. Biochemical Corp. or Amersham Corp. T4 DNA ligase was purchased from Promega. *E. coli* SSB was purchased from Pharmacia Biotech Inc.

DNA Oligomers—Two 30-mer primers, one 80-mer, and two 100-mer templates were used. The primers were annealed to the middle of their templates with equal lengths (25 or 35 nucleotides) of single-stranded DNA overhang on each side. Both 30-mer primers, two 40-mers, and three 50-mers, which were the 3′- and 5′-half of 80-mer and 100-mer templates, respectively, were synthesized on an Applied Biosystems 392 DNA/RNA synthesizer. The 3′-half of a template was 5′-end-phosphorylated by ATP using T4 polynucleotide kinase. The two halves were then annealed to the 30-mer primer and ligated to form the full template. Primers and templates were gel-purified.

The sequences of the 30-mer primer/80-mer template were as follows.

```
                                        5′AG GAG GTT TAG TAC CGC
3′ GGC CTT ATC CAC ATA GTG GCA TGA GTC CTC CAA ATC ATG GCG

   CAC CCT TAG AAC C 3′
   GTG GGA ATC TTG GCG GTG GGA GTC TTG GCG GTG GGA GT 5′
```

SEQUENCE 1

The sequences of the 30-mer primer/100-mer templates were as follows.

```
                                                      5′ G TAC CGC
3′  GGC CTT ATC CAC ATA GTG GCA TGA GTC C T C CAA ATC ATG GCG

   CAC CCT TAG AAC CGG TGT TTG GT 3′
   GTG GGA ATC TTG GCC ACA AAC CAT TTT G⟨C/A⟩T GTC TGT GAC TCG TTC

   AGG CTA TTA CTG A 5′
```

SEQUENCE 2

G is the target site where misincorporation frequencies are measured. The next nucleotide downstream from the target G is either C or A.

Nucleotides—dNTP substrates were purchased from Pharmacia Biotech Inc. [γ-^{32}P]ATP (4500 Ci/mmol) was purchased from ICN Radiochemicals.

Methods

Primer Labeling Reaction—The primer was 5′-end-labeled with ^{32}P using T4 polynucleotide kinase in enzyme reaction buffer at 37 °C for 60 min. p/t DNA was annealed in enzyme reaction buffer using a ratio of 1 primer to 1.2 templates by heating to 90 °C and gradually cooling to room temperature. The concentration of p/t DNA after annealing was 100 nM (primer terminus).

Processive Synthesis on 30-Mer/100-Mer p/t DNA—p/t DNA and ATP were incubated at 37 °C with different combinations of accessory proteins (β, γ complex) and SSB in 20 μl of enzyme reaction buffer containing 4% glycerol for 4 min; then, 10 μl of enzyme reaction buffer containing 4% glycerol, four dNTPs, and pol III core was added to start the reaction. Reactions were run for 3 min at 37 °C and quenched by adding 60 μl of 20 mM EDTA in 95% formamide (F/E) to the reaction mixture. Final concentrations in the reactions were 5 nM p/t, 5 nM pol III core, 167 μM ATP, 133 μM dATP, 133 μM dCTP, 133 μM dGTP, 133 μM dTTP, and the accessory proteins, if present, were 20 nM γ complex, 80 nM β_2, 320 nM SSB.

Primer Extension Reactions—Primer extension reactions were carried out using pol III core, pol III holoenzyme, α subunit, and α holoenzyme. All reactions were carried out in a similar way. Time courses were run prior to kinetics experiments to determine conditions for measuring incorporation opposite a target site.

Three solutions were made for measurements using pol III core in the presence of β, γ complex and SSB. Solution A contained 15 nM p/t, 60 nM γ complex, 240 nM β_2, 960 nM SSB, and 4% glycerol in enzyme reaction buffer. Solution B consisted of enzyme reaction buffer containing 0.5 mM ATP and varied concentrations of the dNTP to be incorporated opposite target site. Solution C contained 15 nM of pol III core, 150 μM running start dATP, and 4% glycerol in enzyme reaction buffer. The reaction was performed as follows: 5 μl of solution A was first mixed with 5 μl of solution B and incubated at 37 °C for 4 min to allow the γ complex to load β sliding clamp onto the DNA; then 5 μl of solution C was added to the A + B mixture to initiate the primer extension reaction. The concentrations in the final 15-μl reaction mixture were 5 nM p/t, 5 nM pol III core, 20 nM γ complex, 80 nM β_2, 320 nM SSB, 167 μM ATP, 50 μM dATP, and varied concentrations of the dNTP to be incorporated opposite the target site.

Reactions were run at 37 °C for 6 min for misincorporation opposite a target site. This constituted a multiple completed hit (MCH) condition in which about 50% of the primers were used (see the "Appendix" (60)). For correct incorporation opposite the target site, 3 nM pol III core was present in solution C to give 1 nM in the final reaction, and the reactions were run for 1 min at 37 °C, creating single completed hit (SCH) conditions, in which about 10% of the primers were utilized. Reactions were quenched by adding 30 μl of F/E to the reaction mixture. The samples were heated to 100 °C for 6 min, placed on ice for 3 min, then loaded on a 16% polyacrylamide denaturing gel. The gel was run at 2000 V for 3 h to separate reaction products.

Primer extension reactions by α subunit in the presence of β, γ complex and SSB were carried out similarly using 8 nM α subunit instead of pol III core polymerase in 6 min reactions for misincorporation (MCH conditions, 50% of primers used) and 2 nM α subunit in 1 min reactions for correct incorporation opposite the target site (SCH conditions, 10% of primers used). Primer extension by α subunit or pol III core without accessory proteins were done with 8 nM α subunit or 5 nM of pol III core for misincorporation and 1 nM α subunit or 0.5 nM of pol

III core for correct incorporation opposite the target. Also, ATP was omitted from solution C, and the incubation of the A + B mixture was reduced to 1 min. Reactions by α subunit and by pol III core were run for 30 min for misincorporation (MCH condition) and 1 min for correct incorporation (SCH condition). 30-Min reactions utilized about 90% of the primers, while 1-min reactions utilized 10% of the primers.

Fidelity of Pol III Holoenzyme in the Presence of Rescue Nucleotide—Experiments were identical to primer extension reactions with core holoenzyme, except that the concentration of rescue nucleotide, dCTP, was 3-fold greater in solution C than its final concentration in the assay. Misincorporation and correct incorporation reactions were both carried out with 5 nM pol III core and were run for 6 min (MCH condition, 50% of primers used). Misincorporation of the running start nucleotide, dAMP, opposite the target site and beyond was not detected for concentrations up to 100 μM dATP, in the absence of other nucleotides.

Kinetic Analysis—A gel fidelity analysis, outlined in Fig. 1, was used to determine the kinetics of incorporation of each of the four dNTPs opposite the target site as a function of dNTP concentration (20, 26, 27). Integrated polyacrylamide gel band intensities were measured on a PhosphorImager using ImageQuant software (Molecular Dynamics, Sunnyvale, CA). The nucleotide incorporation rate opposite a target site, in either the presence or absence of proofreading exonuclease activity, can be obtained by measuring $I^{\Sigma}_{\mathbf{T}}/I_{\mathbf{T-1}}$, where $I^{\Sigma}_{\mathbf{T}}$ is the integrated gel band intensities of primers extended to the target site and beyond, and $I_{\mathbf{T-1}}$ is the integrated gel band intensity of primers extended to the site just prior to the target site (20, 26).

A plot of the relative incorporation rate, $I^{\Sigma}_{\mathbf{T}}/I_{\mathbf{T-1}}$ as a function of dNTP substrate concentration results in a rectangular hyperbola whose slope in the initial linear region is the apparent V_{max}/K_m. Apparent K_m and relative V_{max} values (20, 26) were obtained using a least squares fit to the rectangular hyperbola. The relative V_{max} value is equal to the maximum value of $I^{\Sigma}_{\mathbf{T}}/I_{\mathbf{T-1}}$. In reactions where misincorporation opposite the target site was relatively inefficient, plots of $I^{\Sigma}_{\mathbf{T}}/I_{\mathbf{T-1}}$ *versus* dNTP concentration showed little or no curvature, and apparent V_{max}/K_m values were obtained by a least squares fit of the data to a straight line. Apparent V_{max}/K_m values that were obtained under MCH conditions were corrected to SCH conditions (see the "Appendix" (60)). The misincorporation efficiency, f_{inc}, which is the inverse of the fidelity, is given by the ratio,

$$f_{inc} = \text{fidelity}^{-1} = \frac{(V_{max}/K_m)_W}{(V_{max}/K_m)_R} \qquad \text{(Eq. 1)}$$

where the subscripts W and R refer to wrong and right incorporations, respectively. Measurement errors for V_{max}/K_m are ± 30% and for f_{inc} are ± 40% (one S.D.).

Dissociation Rate and Cycling of Pol III Core on p/t DNA in the Presence of β, γ Complex—2 nM 30-mer/100-mer DNA was preincubated for 3 min with 100 nM β_2, 20 nM γ complex, 300 nM SSB in the presence of 1 mM ATP, and 0.4 mM dGTP, 0.4 mM dTTP, which are the nucleotides at the 3′-end of the primer. 10 nM pol III core was then added to the mixture to allow formation of pol III holoenzyme on the p/t DNA. Because dATP was not present, an idling reaction occurred in which dTMP and dGMP could be removed and then added back on to the 3′-end of the primer, preventing degradation of the 5′-^{32}P-labeled primer. In a second tube, 500 nM unlabeled 30-mer/80-mer p/t DNA (trap DNA) was preincubated for 3 min with 4.5 μM β_2, 1 μM γ complex, 10 μM SSB, 1 mM ATP in the presence of 0.4 mM dGTP, 0.4 mM dTTP, and 0.6 mM dATP. The contents of the pol III holoenzyme (5 μl) and trap preincubation mixture (containing dATP) (10 μl) were then immediately combined, and four separate reactions were carried out in which 5 μl of dCTP of 1.6 mM, the nucleotide to be incorporated opposite the target G site, was added at delay times of 0, 10, 20, and 40 s. The reaction products were separated by polyacrylamide gel electrophoresis and the proportion of DNA extended beyond the target site was graphed as a function of delay time. A band at the T+2 site was caused by misincorporation at the target site and was not considered true extension, because its intensity was independent of whether dCTP was added (see Fig. 3*A*). The same general procedure was used to measure pol III dissociation at the **T−1** site for M13 DNA and a 30-mer/209-mer p/t DNA, where the 209-mer template was a restriction fragment of M13 DNA. The procedure was modified for the full-length circular M13 DNA as follows: an unlabeled primer (30-mer) was annealed to the M13 DNA downstream of the ^{32}P-labeled primer to form a 60-nt gap; SSB was not present in the reaction and trap solutions.

The effectiveness of the unlabeled 30-mer/80-mer DNA trap was demonstrated by adding pol III core plus β, γ complex, dNTPs and ATP first to the trap and then mixing with the radioactive labeled p/t DNA, followed by the delayed addition of dCTP. The trap was found to be effective over the entire length of the experiment, because negligible DNA synthesis (<1%) occurred on the labeled p/t DNA (data not shown).

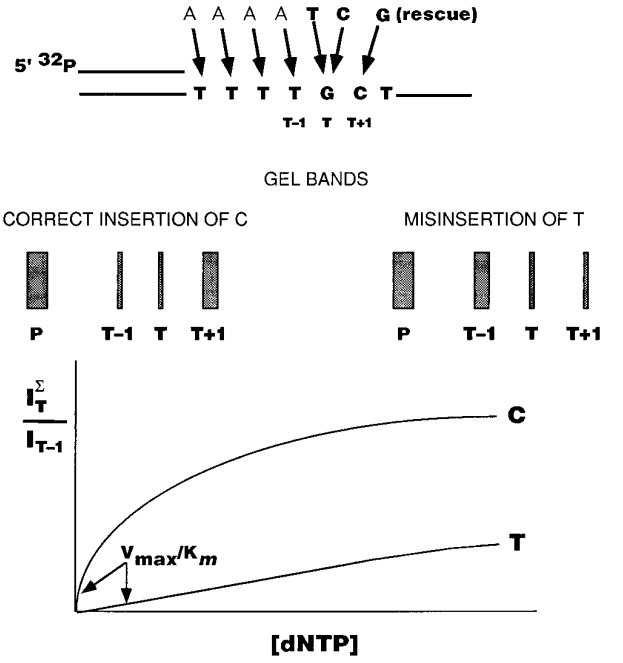

FIG. 1. **Gel kinetic measurement of DNA polymerase fidelity.** Incorporation of wrong (*e.g.* dTMP) or right (dCMP) nucleotides is measured over a broad range of substrate concentrations. Measurements for each of the four dNTP substrates are carried out in separate reactions in which a ^{32}P-labeled primer is extended in a running start (26, 36) by the addition one or more nucleotides to reach a template site, **T−1**, followed by insertion of either a wrong or right nucleotide at a target site, **T**. Three competing events occur following insertion at **T**: (i) the newly inserted nucleotide is excised, returning the primer to **T−1**; (ii) incorporation of one or more next correct (rescue) nucleotides, if present in the reaction, extends the primer to **T+1**, **T+2**, . . . ; or, (iii) the polymerase dissociates creating a band terminating opposite **T**. The primer extension bands are resolved by polyacrylamide gel electrophoresis, and the intensity of each band (*i.e.* $I_{\mathbf{T-1}}$, $I_{\mathbf{T}}$ $I_{\mathbf{T+1}}$, $I_{\mathbf{T+2}}$, etc.) is measured by integration of Phosphorimager tracings (see "Methods"). The rate of insertion of right or wrong nucleotides at site **T** is given by the ratio of gel band intensities: $I^{\Sigma}_{\mathbf{T}}/I_{\mathbf{T-1}}$, where $I^{\Sigma}_{\mathbf{T}} = I_{\mathbf{T}} + I_{\mathbf{T+1}} + I_{\mathbf{T+2}} +$ . . . Apparent V_{max}/K_m is calculated from the slope of the linear region of a plot of this ratio *versus* dWTP or dRTP concentration, where W and R refer to wrong or right incorporations, respectively. The nucleotide misincorporation efficiency, f_{inc}, is the inverse of the fidelity and is given by the ratio of $(V_{max}/K_m)_W$ to $(V_{max}/K_m)_R$, as in Equation 1.

Utilization of multiple p/t DNA molecules by pol III (*i.e.* cycling) was assayed by measuring the increase in the fraction of primer DNA extended as a function of time. Time course reactions were carried out with 20 nM 30-mer/100-mer using two concentrations of pol III holoenzyme (1 and 3 nM) in the presence of all four dNTPs (each at 500 μM). The procedure used was the same as in the primer extension reaction (see above).

RESULTS

A gel kinetic assay (26, 28) designed to measure DNA polymerase fidelity at arbitrary template sites in the absence of proofreading was recently generalized for use with polymerases that can proofread (20). The assay is described above (see "Experimental Procedures") and illustrated in Fig. 1. A more detailed description is contained in Refs. 20 and 27 and an important extension of it is given in the "Appendix" (60).

Three experimental criteria must be satisfied to measure the fidelity of a holoenzyme using this assay: (i) the holoenzyme must be processive on the p/t DNA used in the assay; (ii) primer extension bands attributable to the core enzyme (without processivity proteins) must be negligible compared with holoen-

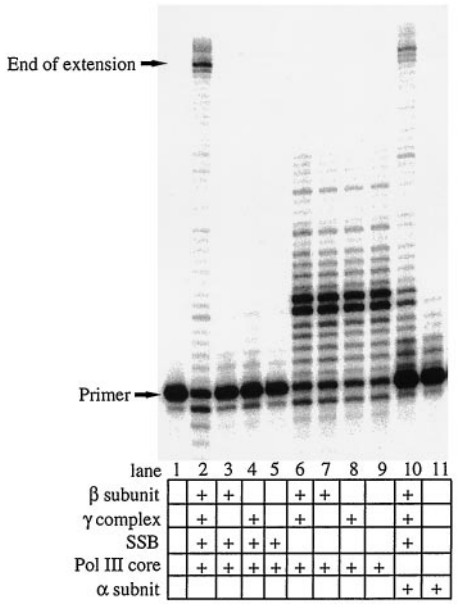

FIG. 2. **Requirements for processive DNA synthesis by pol III core and α holoenzymes on a 30-mer/100-mer p/t DNA.** Primer extension reactions by pol III core (5 nM) (*lanes 2–9*) or α subunit (5 nM) (*lanes 10* and *11*) were performed on a 30-mer/100-mer p/t DNA at 37 °C, for 3 min, in the presence of different combinations of accessory proteins, β (80 nM, as a dimer), γ complex (20 nM), and SSB (320 nM, as a monomer), and were analyzed by denaturing (8 M urea) polyacrylamide gel electrophoresis. A 30-mer primer was annealed to a 100-mer template to create 5′- and 3′-template single-strand overhangs, 35 nt long. All reactions contain 5 nM DNA, 0.17 mM ATP, 133 μM dATP, dCTP, dGTP, and dTTP, 8 mM $MgCl_2$, 50 mM NaCl, 40 μg/ml bovine serum albumin, 5 mM dithiothreitol, and 20 mM Tris-HCl, pH 7.5. *Lane 1* contains p/t DNA only.

zyme-catalyzed extension bands; (iii) primer extension bands attributable to the holoenzyme must arise either from SCH, in which an enzyme encounters a given p/t DNA at most once and then dissociates, or alternatively from MCH, in which enzymes encounter and dissociate from a given p/t DNA multiple times; primer extension bands caused by incompleted hits, arising if an enzyme remains bound at the primer-3′ terminus when the reaction is terminated, must be negligible. All three criteria are satisfied in our system, as demonstrated in the next two subsections. A detailed mathematical analysis of the effects of SCH and MCH on the fidelity measurements is given in the "Appendix" (60).

Processive Synthesis by Pol III Holoenzyme on Short, Synthetic p/t DNA—On large DNA templates, such as φX and M13, pol III core polymerase typically incorporates between 10 and 20 nucleotides per binding event (16), while pol III core plus β and γ complex (pol III holoenzyme) incorporates more than 5000 nucleotides per binding event (8, 14). This difference implies that the processivity proteins (β, γ complex) increase the time pol III core remains bound to p/t DNA by 2 to 3 orders of magnitude.

We have recently shown that a DNA template as small as 80 nucleotides in length, annealed to a 30-mer primer, supports processive synthesis by pol III holoenzyme in the presence of SSB (29). The SSB protein, although useful in eliminating secondary structure that can cause polymerase pausing, is generally not required for processive synthesis on long, closed circular DNAs such as bacteriophage φX or M13. In our 30-mer/100-mer or 30-mer/80-mer (29) constructs, however, SSB is required, perhaps to prevent the β clamp from sliding off the end of the template before it has had time to associate with a polymerase molecule.

Fig. 2 illustrates the requirements for processive synthesis in our systems. Synthesis by pol III core is essentially nonprocessive on the 30-mer/100-mer p/t DNA (Fig. 2, *lane 9*). The addition of β or γ complex, alone or together, has little effect; the enzyme still fails to reach the end of the template strand and dissociation bands are evident at each template position (Fig. 2, *lanes 6–8*). SSB alone strongly inhibits core polymerase, even in the presence of either β or γ complex (Fig. 2, *lanes 3–5*). However, when β, γ complex and SSB are all present in the reaction, synthesis proceeds processively, reaching the end of the 100-mer template (Fig. 2, *lane 2*). Note that dissociation bands characteristic of the core enzyme (Fig. 2, *lanes 6–9*) are strongly attenuated during holoenzyme synthesis in the presence of SSB (Fig. 2, *lane 2*). The α subunit lacks the ε proofreading 3′-exonuclease of pol III core and is lower in polymerase activity than pol III core, but its requirements for processive synthesis are similar. On its own, it cannot replicate to the end of the 100-mer template (Fig. 2, *lane 11*) but in the presence of β, γ complex and SSB it becomes much more processive (Fig. 2, *lane 10*).

Dissociation Rate and Cycling of Pol III Holoenzyme on p/t DNA—Despite their high processivity, the pol III and α holoenzymes eventually dissociate from p/t DNA. We measured the lifetime of pol III holoenzyme on p/t DNA using three different templates: a 100-mer, a 209-nt restriction fragment of M13 DNA, and full-length circular M13 DNA. Pol III holoenzyme was loaded onto a labeled p/t DNA in the presence of dGTP and dTTP allowing the polymerase to idle. Next, dATP was added along with a large excess of unlabeled trap DNA, and the reaction was allowed to incubate for varying "delay" times before addition of dCTP allowed processive synthesis. For each p/t DNA, the fraction of extended primer decreased with increasing delay times, exhibiting a good fit to an exponential decay (Fig. 3*A*). The lifetimes ($t_{½}$ values) of the pol III-β-p/t complexes are 4.7 s for the 100-mer, 25 s for the 209-nt M13 fragment, and 46 s for the full-length M13 DNA (Fig. 3*A*).

Cycling of pol III holoenzyme is apparent from the level of primer utilization over time. In the extreme, if enzymes fail to dissociate from p/t DNA, the fraction of extended primers would saturate at the pol/DNA ratio. We measured an exponential increase in primer utilization over time using molar ratios of pol/DNA of 1/20 and 3/20. In both cases, ~80–90% of the primer was converted to product DNA with characteristic times ($t_{½}$) of 4 and 2 min for the lower and higher ratios, respectively (Fig. 3*B*).

These measurements indicate that the lifetime of pol III holoenzyme on our p/t DNA is much shorter than the reaction times used for pol III holoenzyme fidelity measurements (typically 1–6 min), justifying the assumption that gel bands arise from (single or multiple) completed hits between enzyme and p/t DNA.

Increased Processivity Facilitates Multiple Misincorporations—A qualitative assessment of nucleotide misincorporations by pol III core and holoenzyme was made by using only two substrates (dGTP and dCTP) to copy the synthetic 30-mer/80-mer p/t DNA (Fig. 4). When pol III core is present at low concentration (1 nM), primer extension is essentially stopped by the first template T in 2-min reactions (Fig. 4*D*). In longer reactions (>4 min), a small amount of primer extension beyond the first template T indicates a misincorporation event at the first template T site (presumably dGMP·T). Extension beyond the first template A is not observed even after 64 min. Using a 10-fold higher concentration of pol III core (10 nM), misincorporation opposite the first template T is clearly observed in a 2-min reaction, while extension opposite and beyond the next template A site is only detectable for incubation times of 16 min or longer (Fig. 4*C*). By contrast, multiple misincorporations are

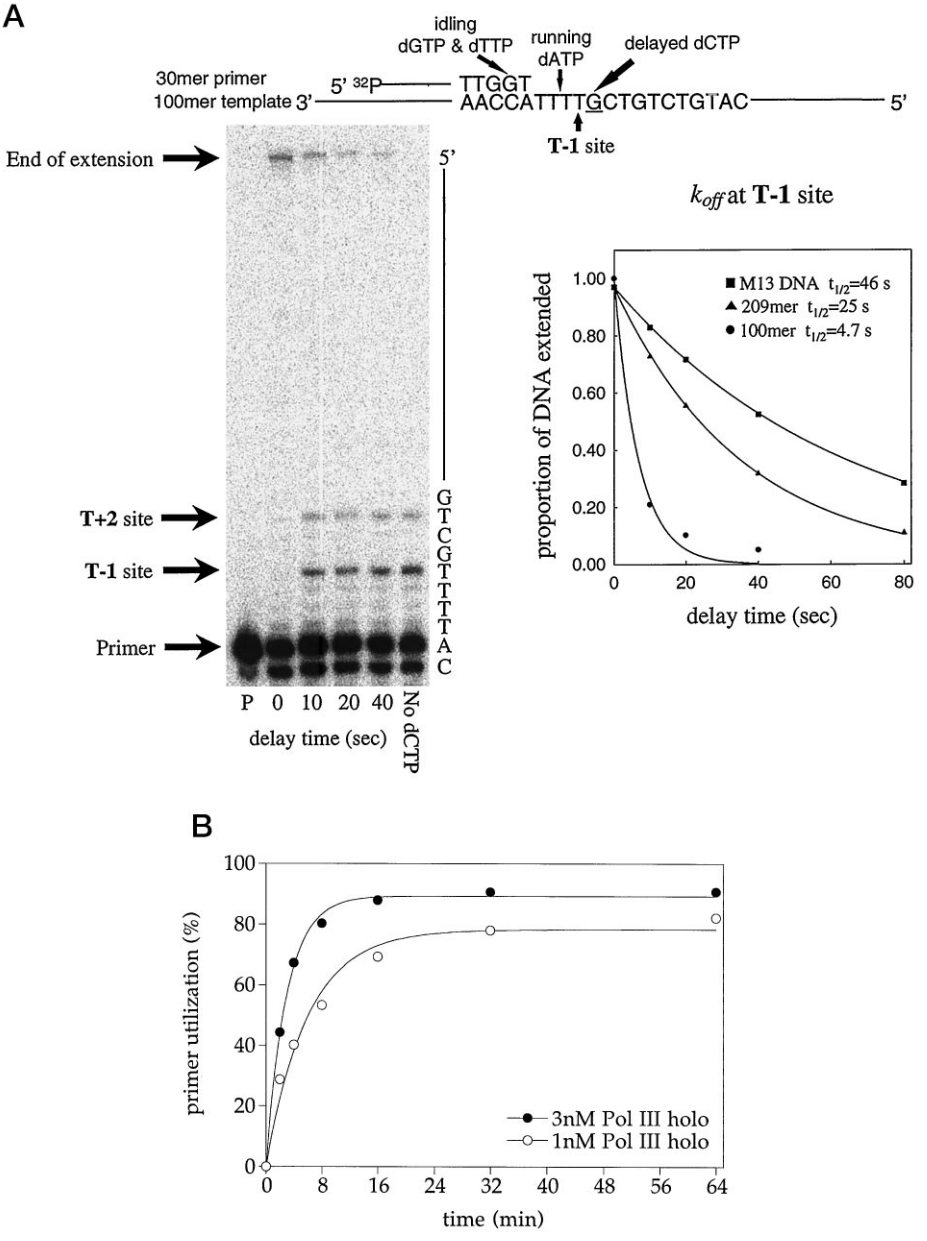

FIG. 3. **Pol III holoenzyme dissociation and recycling rates on p/t DNA.** *A*, dissociation of pol III holoenzyme was measured on p/t DNA using three different templates: a 100-mer, a 209-nt restriction fragment of M13 DNA and full-length circular M13 DNA. Pol III core was preincubated with β_2,γ complex, SSB and p/t DNA in the presence of idling dGTP and dTTP. Running start dATP was added to the reaction along with an excess of trap DNA (also preincubated with β_2,γ complex and SSB) to sequester free/dissociated enzyme. After a variable delay time, dCTP was added and, 10 s later, the reactions were stopped. For the lane designated "no dCTP" the reaction was stopped 80 s after the addition of dATP and trap DNA (dCTP was never added). The *gel* on the *left* shows data from experiments with our standard 30-mer/100-mer p/t, sketched at the *top*. The lifetime k_{off} (*i.e.* $t_{½}$) was measured from the decrease in the proportion of DNA extended beyond the target site (see "Methods"). *Plots* on the *right* summarize the data for all three primer/templates. The *solid lines* are least squares fits to a simple exponential decay, with half-lives as indicated. *B*, 20 nM 30-mer/100-mer p/t DNA was extended by pol III holoenzyme at 37 °C for different reaction times and different enzyme concentrations with all four dNTPs available (500 μM). Primer utilization was measured as percentage of total DNA and plotted against time. *Solid lines* are least squares fits to an exponential function. *Open circles*: 1 nM pol III holoenzyme, $t_{½}$ = 4.1 min, maximum utilization = 78%. *Solid circles*: 3 nM pol III holoenzyme, $t_{½}$ = 2.0 min, maximum utilization = 89%.

catalyzed by pol III holoenzyme (Figs. 4, *A* and *B*). Seven additional misincorporations at template T and A sites are observed downstream of the initial T misincorporation site, including consecutive misincorporations opposite two adjacent T sites.

The absence of discernible primer extension bands directly opposite or beyond the first template T site in the 1 nM pol III core reactions shows that the enzyme either fails to misinsert either G or C opposite T or removes all misinserted nucleotides prior to dissociation. The low intensity or complete absence of pause bands opposite the template T and A sites in the pol III holoenzyme reactions where misincorporation occurs indicates that the holoenzyme, having created a mismatch, tends to either excise a misincorporated dNMP or insert the next correct nucleotide rather than dissociate at the misincorporation site.

The fact that misincorporations occur readily in the presence of β, γ complex does not imply that fidelity of DNA synthesis has been impaired. Rates of incorporation of right as well as wrong nucleotides are increased relative to polymerase dissociation. To affect fidelity, enhanced processivity must favor one incorporation rate relative to the other. The next set of experiments quantify the effect of β, γ complex on the fidelity of DNA synthesis.

Increased Processivity Has No Measurable Effect on Fidelity in the Absence of Proofreading—We investigated the effect of β, γ complex on the fidelity of α subunit using the 30-mer/100-mer p/t construct (Fig. 5*A*). On this p/t DNA, polymerase must incorporate dAMP opposite T at four running start sites before reaching a G site (target). At the target site, it can either incorporate a dNMP opposite G or dissociate.

For the α subunit alone, the f_{inc} values for misincorporation, dAMP·G, dGMP·G, and dTMP·G are 1.2×10^{-5}, 2.4×10^{-5}, 8.0×10^{-5}, respectively (Fig. 5*A*). The corresponding values for the α holoenzyme are 5.6×10^{-6}, 3.5×10^{-5}, and 1.8×10^{-4}, respectively (Fig. 5*B*). Therefore, the fidelity of the α subunit does not change significantly with increased processivity. The effect of processivity proteins is seen, however, in an overall reduction of the apparent K_m for correct insertions, from 42 to 29 μM (Table I). As expected, the increased lifetime of the polymerase·DNA complex allows more opportunity for binding a dNTP substrate.

Fidelity of Pol III Holoenzyme—The misincorporation effi-

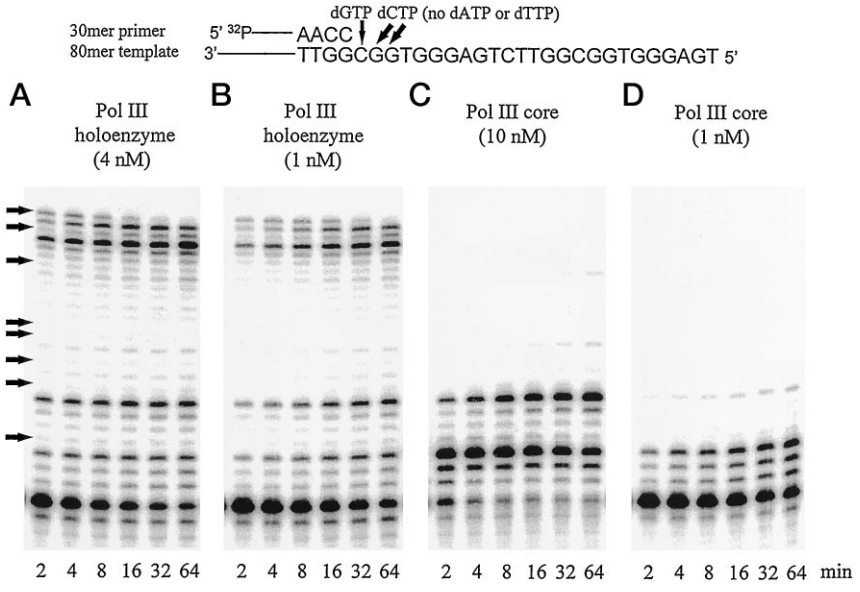

FIG. 4. **Multiple misincorporations catalyzed by pol III core in the presence of β, γ complex processivity proteins.** Primer extension reactions were carried out at 37 °C, for different incubation times and enzyme concentrations, with only two dNTPs present in the reaction, dCTP (120 μM) and dGTP (120 μM). *A*, pol III core (10 nM), β (40 nM, as a dimer), γ complex (5 nM), and SSB (105 nM, as a monomer); *B*, pol III core (4 nM), β (40 nM, as a dimer), γ complex (5 nM), and SSB (105 nM, as a monomer); *C*, pol III core (10 nM); *D*, pol III core (1 nM). The *arrows* indicate where misincorporations have occurred at template A and T sites. A sketch of the p/t DNA (5 nM) is shown above the gels.

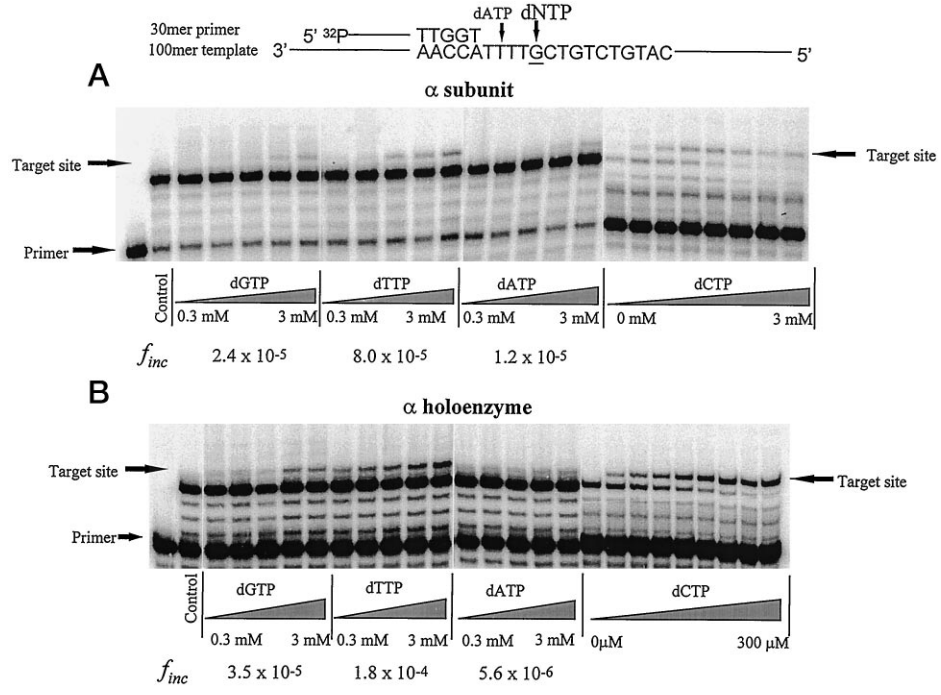

FIG. 5. **Misincorporation efficiencies catalyzed by the pol III α subunit and pol III α holoenzyme.** A running start primer extension reaction at 37 °C incorporates 4 As (opposite T) to reach a template target G. The concentration of each dNTP used for incorporation opposite the target G was varied to measure the kinetics of incorporation. *A*, α subunit (8 nM); *B*, α holoenzyme (8 nM α subunit, 80 nM β as a dimer, 20 nM γ complex). The misincorporation efficiency, f_{inc}, in the absence of proofreading, was calculated using Equation 1 (see "Methods"). The lane designated as "*Control*" refers to reactions carried out using the running start substrate, dATP (50 μM), in the absence of the other three dNTPs. The incorporation of dCMP opposite G was run under single-hit conditions (1-min incubation time, 1 nM α subunit, 10% primers used), while the three misincorporation reactions were run under multiple hit conditions (α alone: 30-min incubation time, 8 nM α subunit, 90% primers used; α holoenzyme: 6-min incubation time, 8 nM α subunit, 50% primers used), see the "Appendix" (60). SSB (320 nM) is present in all reactions. A sketch of the p/t DNA (5 nM) is shown above the gels. The nucleotide incorporation rate opposite a target site, in either the absence or presence of proofreading exonuclease activity (see Fig. 6), are obtained by measuring $I_{\mathbf{T}}^{\infty}/I_{\mathbf{T-1}}$, where $I_{\mathbf{T}}^{\infty}$ are the integrated gel band intensities of primers extended to the target site and beyond, and $I_{\mathbf{T-1}}$ is the integrated gel band intensity of primers extended to the site just prior to the target site.

ciencies for the pol III holoenzyme are: dAMP·G = 4.2×10^{-7}, dGMP·G = 3.2×10^{-5}, dTMP·G = 5.6×10^{-6} (Fig. 6*A*). Notice that the dAMP·G misincorporation efficiency of the pol III holoenzyme is more than 13-fold lower than the corresponding value for the α holoenzyme (Figs. 5*B* and 6*A*, *dATP lanes*). Assuming their misinsertion rates are the same, this indicates that the ϵ subunit is able to excise more than 92% of misinserted dAMPs. Similarly, the dTMP·G misincorporation efficiency is 32-fold lower than α holoenzyme (Figs. 5*B* and 6*A*, *dTTP lanes*), indicating that approximately 97% of misinserted dTMPs are excised. A comparison of misincorporation efficiencies for α subunit, α holoenzyme, and pol III holoenzyme is given in Table I.

Misincorporation of dGMP opposite G by pol III holoenzyme presents an interesting anomaly. In this case, the pol III holoenzyme misincorporation efficiency is between 1 and 2 orders of magnitude higher than for the other two mispairs (G·G in Table I, next to last column) and approximately equal to that of the α holoenzyme (G·G in Table I, second data column). Furthermore, the dGTP concentrations required to observe misin-

TABLE I

Misincorporation by α subunit, α holoenzyme (α holo), pol III core, and pol III holoenzyme (pol III holo) without rescue dNTP

dATPdNTP

30-Mer primer 5′ ^{32}P — TTGGT ↓ ↓

100-Mer template 3′ — AACCATTTTGCTGTCTGTAC — 5′

A[a]

Base pair		α subunit	α holo	α holo[a]	Pol III core	Pol III holo	Pol III holo[a]
C · G	f_{inc} (K_m)	1 (0.042 mM)	1 (0.029 mM)	1 (0.010 mM)	1 (0.027 mM)	1 (0.003 mM)	1 (0.001 mM)
A · G	f_{inc} (K_m)	1.2×10^{-5} (>3 mM)	5.6×10^{-6} (>3 mM)	8.0×10^{-6} (>3 mM)	$<10^{-5}$	4.2×10^{-7} (>3 mM)	$<10^{-7}$
G · G	f_{inc} (K_m)	2.4×10^{-5} (>3 mM)	3.5×10^{-5} (2 mM)	3.2×10^{-5} (>3 mM)	$<10^{-5}$	3.2×10^{-5}[b] (0.013 mM)	7.0×10^{-7} (>3 mM)
T · G	f_{inc} (K_m)	8.0×10^{-5} (>3 mM)	1.8×10^{-4} (2.3 mM)	1.4×10^{-4} (1.8 mM)	$<10^{-5}$	5.6×10^{-6} (1.4 mM)	5.8×10^{-4}[b] (0.001 mM)

[a] The base after the target G site was changed from C to A.

[b] Pol III holoenzyme misincorporation efficiencies for which the target nucleotide was also the rescue nucleotide were calculated by comparison with correct incorporation in the presence of similar amounts of rescue nucleotide.

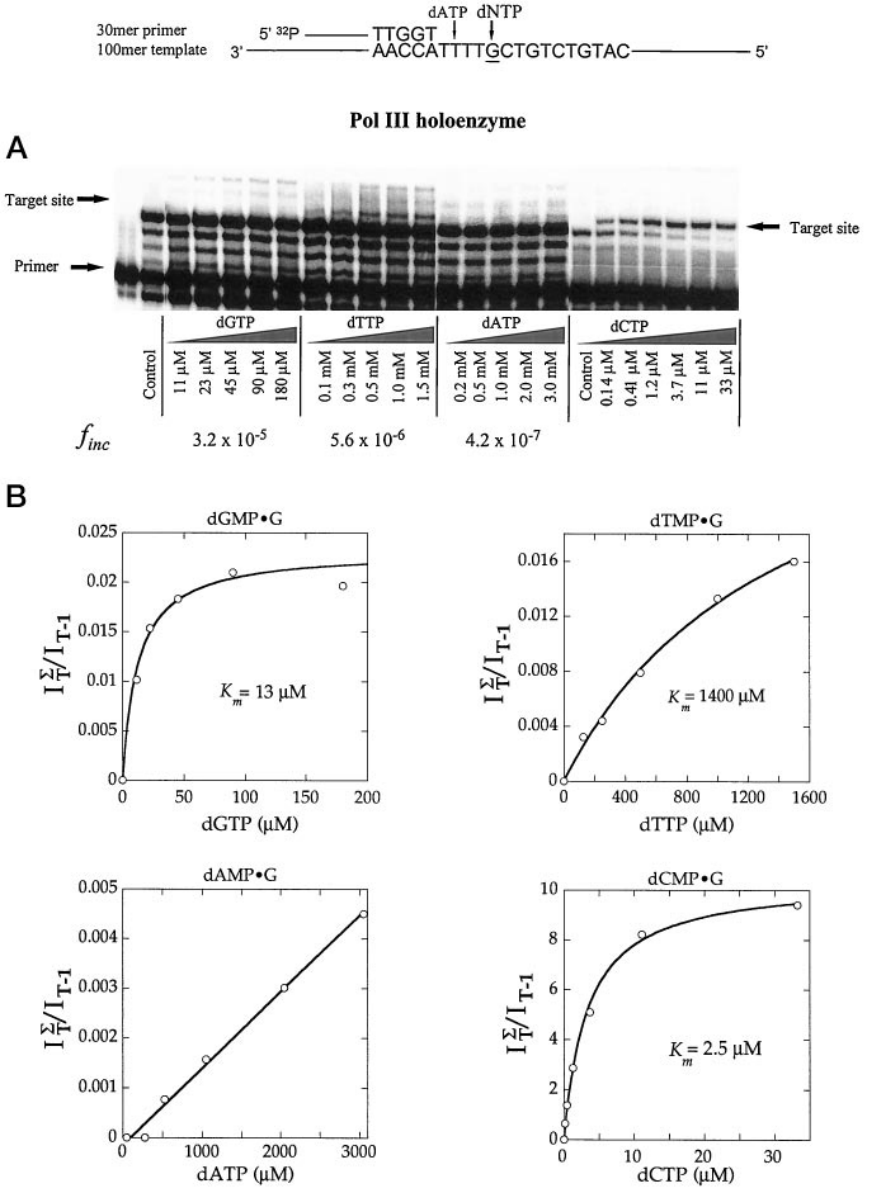

FIG. 6. **Misincorporation efficiencies catalyzed by the pol III holoenzyme.** Four As were incorporated in a running start primer extension reaction, at 37 °C, to reach a template target G. The concentration of the four dNTPs were varied individually to measure the kinetics of incorporating wrong (dGMP, dTMP, and dAMP) and right (dCMP) nucleotides opposite G. *A*, pol III holoenzyme (5 nM pol III core, 80 nM β as dimer, 20 nM γ complex); the lane designated as "*Control*" refers to reactions carried out using the running start substrate, dATP (60 μM), in the absence of the other three dNTPs. The incorporation of dCMP opposite G was run under single-hit conditions (1-min incubation time, 1 nM pol III core, 8% primers used), while the three misincorporation reactions were run under multiple-hit conditions (6-min incubation time, 5 nM pol III core, 50% primers used), see the "Appendix" (60). The misincorporation efficiency, f_{inc}, in the absence of rescue nucleotide was calculated using Equation 1; see "Experimental Procedures." Misincorporation efficiency for dGMP·G was calculated by comparison with dCMP·G in the presence of a similar concentration of dGTP rescue nucleotide. *B*, Michaelis-Menten saturation plots of I_T^{Σ}/I_{T-1} as a function of dNTP concentration. The *line* is a least squares fit to either a straight line (dAMP·G) or a rectangular hyperbola (dGMP·G, dTMP·G, dCMP·G): $y = x \cdot V_{max}/(x + K_m)$ with the fitted parameter K_m as written on the graph. Data points at the origin represent reactions run in the presence of running start levels of dATP alone. Running start levels were well below misincorporation levels, as indicated by a second point on the *x* axis in the dATP graph. SSB (320 nM) is present in all reactions. A sketch of the p/t DNA (5 nM) is shown above the gels.

corporation (11–180 μM) are considerably lower than for either dTTP (100 μM to 1.5 mM) or dATP (200 μM to 3 mM) (Fig. 6*A*). The estimated K_m (G·G) ~13 μM for pol III holoenzyme is 100 times lower than K_m (T·G) ~1.4 mM (Fig. 6*B*). In contrast, the value of K_m (G·G) for the α holoenzyme is about 2 mM.

An important clue to the source of this result is that the template base immediately downstream from the target G is C. When the downstream template C is replaced by A (Table I,

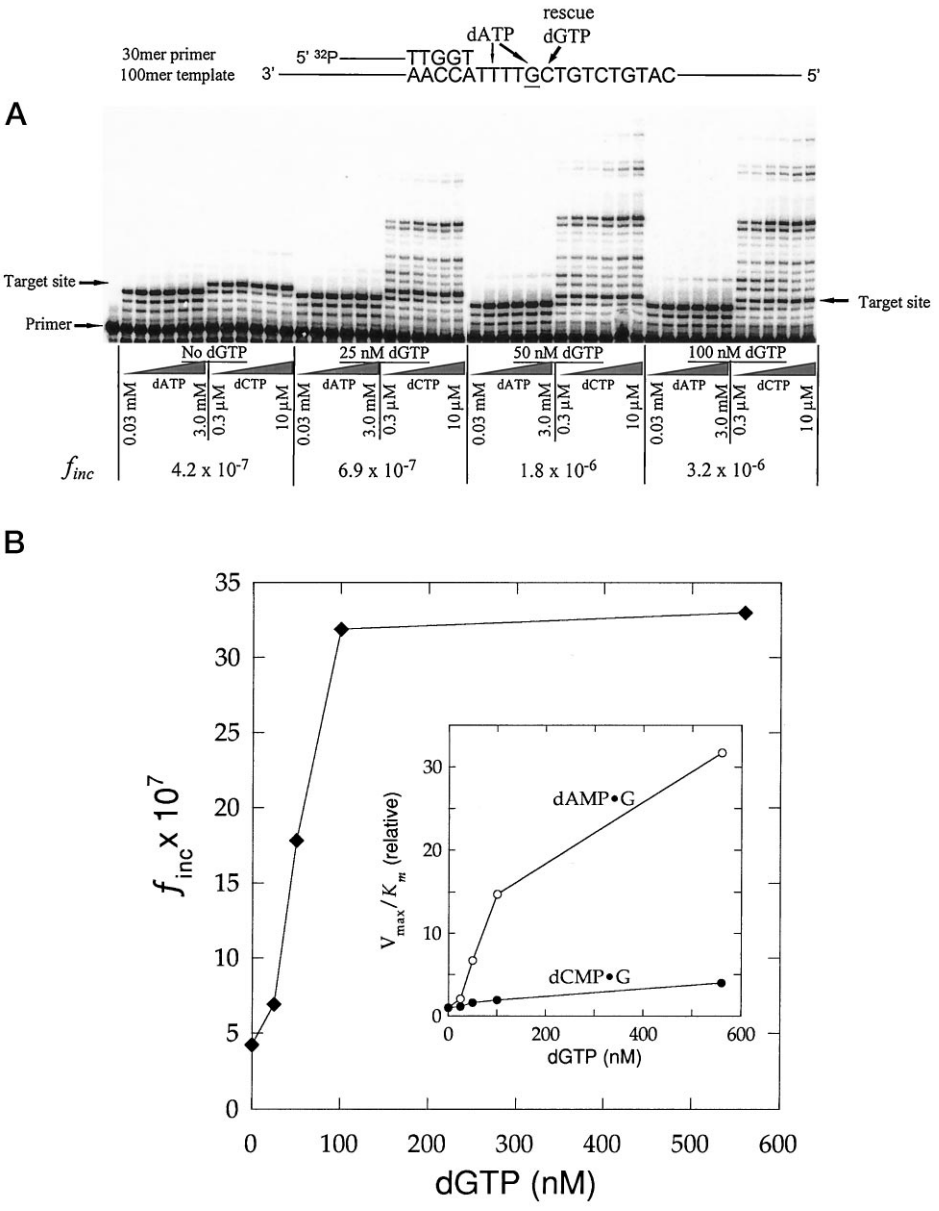

FIG. 7. **Reduction in pol III holoenzyme fidelity with increasing concentration of rescue dGTP.** *A*, misincorporation of dAMP and correct incorporation of dCMP opposite a template target G site in the presence of 0, 25, 50, and 100 nM rescue dGTP; *B*, a plot of the misincorporation efficiency, f_{inc} (Equation 1), as a function of dGTP concentration, derived from the data shown in the *inset*; *Inset*, a plot of V_{max}/K_m values relative to those measured without rescue dGTP (*i.e.* V_{max}/K_m (dGTP $\geq$ 0 nM) divided by V_{max}/K_m (dGTP = 0 nM)) for dAMP·G mispairs and dCMP·G correct pairs in the presence of 0, 25, 50, and 100 nM rescue dGTP. Reaction conditions are similar to those described in the legend to Fig. 6.

last column), the misincorporation frequency f_{inc} (G·G) for pol III holoenzyme decreases by a factor of about 50 (from 3.2×10^{-5} to 7.0×10^{-7}) while f_{inc} (T·G) increases 100-fold (from 5.6×10^{-6} to 5.8×10^{-4}). In contrast, changing the downstream nucleotide has almost no effect on misincorporation by α holoenzyme (Table I, α holo columns).

Fidelity of the Pol III Holoenzyme in the Presence of Rescue Nucleotide—The fidelity of a polymerase that doesn't proofread is independent of the absolute concentration of dNTP substrates (30–32). We assayed the α holoenzyme in the absence and presence of next correct nucleotide and verified that f_{inc} values do not depend on this nucleotide concentration (data not shown). In contrast, the fidelity of a polymerase that proofreads is reduced as the concentration of next correct nucleotide is increased. This "next nucleotide" effect is an important hallmark of polymerases containing an associated proofreading exonuclease (31, 33).

Both correct (dCMP·G) and incorrect (dAMP·G) incorporations increase with increasing concentrations of rescue dGTP (Fig. 7*A*). The relative incorporation rates (normalized to the incorporation rate in the absence of rescue dGTP) are plotted as a function of dGTP concentration in the *inset* of Fig. 7*B*. Increasing concentration of rescue dGTP clearly enhances incorporation of the wrong dNMP (dAMP) more than the right (dCMP). The misincorporation efficiency, f_{inc} (dAMP·G), is plotted in Fig. 7*B*. The misincorporation efficiency for dAMP·G by pol III holoenzyme increases from $f_{inc} = 4.2 \times 10^{-7}$ in the absence of dGTP to 3.3×10^{-6} at 600 nM dGTP. The increase is most pronounced in the 25–100 nM dGTP range and saturates between 100 and 600 nM dGTP.

Overall, an 8-fold reduction in holoenzyme fidelity is seen, attributable to inhibition of proofreading by insertion of a next correct nucleotide. The maximum value of f_{inc} (dAMP·G) = 3.3×10^{-6} for pol III holoenzyme is only 1.7-fold lower than that of the proofreading-deficient α holoenzyme. Assuming misinsertion is the same for the two enzymes, we estimate that 40% of misinserted dAMP's are proofread in the presence of saturating rescue dGTP, compared with more than 92% without rescue.

DISCUSSION

Replicative DNA synthesis by pol III holoenzyme is highly processive (8, 14), with more than 5000-nt incorporated per template binding event. In contrast, synthesis by pol III core is

essentially distributive, with an average of 10–20 nucleotides incorporated (16). Our objective in this paper is to determine the effect of the polymerase accessory proteins, β, γ complex, on the frequency of base substitution errors in the presence and absence of proofreading by the ϵ subunit. This experiment is part of a general inquiry into the biochemical basis for mutagenic hot and cold spots by measuring fidelity in different sequence contexts (34–37). In the process, we have devised a minimal synthetic p/t DNA system that supports processive synthesis by pol III holoenzyme with sequences that can be varied arbitrarily (29). This system, in conjunction with our previously described gel kinetic assay (20), allows quantification of misincorporation efficiencies below 10^{-6}.

Holoenzyme Dissociation and the Gel Kinetic Assay—To use the assay to measure the fidelity of highly processive DNA polymerases it is necessary that the primer extension bands arise predominantly from either single or multiple completed hits, but not from incompleted hits that occur when an enzyme remains bound to the primer. The lifetime data demonstrate that the conditions to achieve either SCH or MCH conditions, as required by the assay, are satisfied. In other words, during the length of time of the pol III holoenzyme fidelity measurements on the 100-mer template, 1-min incubation for incorporation of the right nucleotide (SCH) and 6-min incubations for the wrong nucleotide (MCH), pol III core in the presence of β, γ complex is able to complete the hit by dissociating from the primer terminus with a half-life of about 4.7 s (Fig. 3).

Pol III core can carry out processive DNA synthesis on long templates such as primed full-length circular M13 or ϕX DNA requiring just the presence of β, γ complex. Although SSB stimulates processive DNA synthesis by pol III holoenzyme (9), perhaps by melting of hairpin secondary structures, it is not required for processive synthesis on long p/t DNA constructs. We have shown that processive DNA synthesis also occurs on short synthetic primed oligomer templates, *e.g.* an 80-mer (29) or a 100-mer (Fig. 2) provided that SSB is present in the assay in addition to β, γ complex. SSB may act to inhibit the β clamp from sliding off the end of the short template (29), suggesting that the 4.7- and 25-s lifetimes of pol III on the 100- and 209-nt templates, respectively, are determined primarily by the rates of SSB dissociation from the short template DNA.

The lifetime measurement using M13 DNA (46 s) was carried out in the absence of SSB and is likely to be a true measure of β (or β, γ complex) dissociation. However, it was determined at a specific p/t DNA site. Since we have previously shown that polymerase off rates can differ significantly, *e.g.* on the order of about 10-fold, at different positions along the template (38), the 46-s half-life is shorter than, but not inconsistent with, a previous measurement on ΦX DNA of about 4 min (39).

Pol III Holoenzyme Is a High Fidelity Enzyme—The misincorporation frequencies for the α subunit and α holoenzyme, neither of which can proofread, are on the order of 10^{-4} for dTMP·G mispairs and 10^{-5} for dAMP·G and dGMP·G mispairs (Table I). These values are similar to earlier kinetic estimates (40), suggesting that base selection by α contributes a factor of roughly 10^4-10^5 to the fidelity of genome duplication. Our measurements have focused on base substitutions. Another recent study has shown that -1 frameshift errors catalyzed by α subunit alone, in a gap filling assay measuring mutations in the *lacI* gene, may be occurring with about a 70-fold higher frequency than base substitution errors (41).

The misincorporation frequencies for the proofreading proficient pol III holoenzyme were 5.6×10^{-6} for dTMP·G mispairs and 4.2×10^{-7} and 7.0×10^{-7} for dAMP·G and dGMP·G mispairs, respectively, in sequences for which primer-template misalignments cannot readily occur (Table I). In a series of papers by Fersht and co-workers (33, 42–45), pol III holoenzyme misincorporation frequencies were determined by measuring the reversion of defined single-site bacteriophage ϕX mutations; the observed values were also typically between 10^{-6} and 10^{-7}.

Effects of Processivity Subunits on Fidelity—The α subunit and the α holoenzyme exhibit similar fidelities (see "Results"; Fig. 5 and Table I). Although the residence time of polymerase at the **T−1** site can limit the insertion rate, the limitation is the same for both right and wrong dNTP substrates and therefore has no effect on fidelity (5, 46). Furthermore, since the α subunit has no capacity for proofreading, its residence time at a target site **T** does not affect incorporation. Mathematically, the fidelity depends on the rate constants for insertion, dissociation, and excision (Equation 5 in the "Appendix" (60)) such that, in the absence of exonuclease activity, the polymerase dissociation rates simply cancel out of the ratio.

Of course, processivity proteins can have effects other than just increasing processivity, see, *e.g.* dNTP-stabilized misalignment, below. In another experiment, the interaction of the thioredoxin processivity protein with exonuclease-deficient bacteriophage T7 pol has been observed to alter base substitution and frameshift mutation rates (18). But processivity *per se* cannot alter nucleotide incorporation fidelities in the absence of proofreading. For processivity to influence polymerase fidelity, the polymerase must be able to proofread.

When a polymerase can proofread, its ability to do so can be hampered if it tends to dissociate from the target site. The effect is small when the correct nucleotide is inserted at the target site, since exonuclease is not very active in this case (47–49). But when an incorrect nucleotide is inserted at the target site, an increased processivity can significantly increase the likelihood of excision. Mathematically, increased processivity means the rate of disocciation becomes smaller relative to the rate of excision and, overall, proofreading is increased. Since the effect is more significant for the wrong nucleotide than for the right nucleotide, the result is fewer misincorporations, *i.e.* higher fidelity. This important point can be demonstrated formally by expressing the fidelity as a function of the relevant rate constants, k_{pol}, k_{exo}, k_{res} and k'_{off} (the rate of dissociation of polymerase from the p/t DNA), see Equation 5 in the "Appendix" (60). This equation can be used to show that the fidelity increases monotonically with decreasing polymerase dissociation rate.

In general, the efficiency of misincorporation, f_{inc}, is expected to (i) increase with increasing concentrations of the next correct (rescue) dNTP and (ii) decrease with increasing processivity. Our results confirm the first point, as discussed in the next section, but are currently inconclusive regarding the second. We attempted to compare the fidelities of pol III core and pol III holoenzyme, but encountered difficulties caused by the extremely poor processivity of pol III core. Poor processivity leads to a large apparent K_m and, thus, a low V_{max}/K_m for incorporation, right or wrong. We find incorporation of dCMP opposite G by pol III core has $V_{max}/K_m = 0.14\ \mu M^{-1}$ (data not shown), compared with $3.7\ \mu M^{-1}$ for pol III holoenzyme (Fig. 6*B*). Since f_{inc} is computed from the ratio of wrong to right V_{max}/K_m, a 26-fold lower value for the right nucleotide leads to a similar reduction in the sensitivity of assay. If the lowest misincorporation efficiency measured with pol III holoenzyme (f_{inc} (A·G) = 4.2×10^{-7}, Table I) represents the limit of sensitivity for the assay, then misincorporation efficiencies for pol III core would have to be $>10^{-5}$ to be detected (Table I, column 5). This high threshold for f_{inc} prevented us from measuring the fidelity of pol III core. Thus, it is possible that the misincorporation efficiencies of pol III core fall below the sensitivity of our assay

even though they may be higher than those of pol III holoenzyme.

Proofreading and the Next Nucleotide Effect on Fidelity—The next nucleotide effect is an important hallmark of polymerases containing an associated proofreading exonuclease. Polymerization is increasingly favored over proofreading as the concentration of rescue dNTP is increased. Our data show an overall 8-fold decrease in fidelity as the rescue nucleotide is increased from 0 to 600 nM dGTP (Fig. 7*B*).

The concentrations of rescue nucleotide required to suppress proofreading are surprisingly low. The effect saturates at 100 nM rescue nucleotide. However, although the reduction is significant, proofreading is not shut off, even after the effect of rescue dNTP has saturated (31) (Fig. 7*B*). The maximum misincorporation efficiency of the pol III holoenzyme in the presence of rescue dNTP, f_{inc} (A·G) ~ 3.3×10^{-6} (Fig. 7*B, inset*) remains less than that of the α holoenzyme, f_{inc} (A·G) = 5.6×10^{-6} (Table I).

Pol III holoenzyme generally exhibits greater fidelity than α holoenzyme. The values of f_{inc} for the α holoenzyme are at most 13-, 32-, and 47-fold greater than for the pol III holoenzyme for dAMP·G, dTMP·G, and dGMP·G, respectively (Table I). If the misinsertion efficiencies are approximately the same for the two enzymes (the α polymerase subunit is common to both processive holoenzymes), then these observations imply that approximately 92% of the misinserted dAMPs, 97% of misinserted dTMPs, and 98% of misinserted dGMPs are excised by pol III holoenzyme in the absence of rescue nucleotide. The 8-fold decrease in fidelity in the presence of saturating rescue nucleotide similarly implies a reduction to 40% of misinserted dAMPs being excised. This proofreading behavior of the pol III holoenzyme agrees with earlier observations on the specificity and mechanism of the ϵ subunit assayed alone or as part of the pol III core (50). However, an important caveat is that it is formally possible that the presence of the ϵ subunit could improve polymerase selectivity for reasons unrelated to mismatch editing. Although this possibility may seem unlikely, ruling out ancillary effects of ϵ on nucleotide selection would require testing an intact holoenzyme containing an ϵ subunit that had been mutationally inactivated.

An anomalously high misincorporation efficiency is measured for the pol III holoenzyme when the target dNTP is also the rescue nucleotide, exemplified by dGMP·G in our original sequence context (f_{inc} = 3.2×10^{-5}, Table I, data column 5), which is almost as high as that for the α holoenzyme, f_{inc} = 3.5×10^{-5} (Table I, data column 2). An explanation may be that the template base C, immediately downstream from the target G, directs the correct incorporation of dGMP on a misaligned p/t DNA. The dGMP·G mutational hotspot disappears when the downstream template C is replaced by an A, and a new dTMP·G hotspot appears (Table I, last column). On this template then, dTMP may be "correctly" incorporated opposite the downstream A on a misaligned p/t DNA. The exceedingly low K_m values accompanying the formation of the two mispairs, K_m (G·G) = 0.013 mM (Fig. 6*B*, Table I, data column 5) and K_m (T·G) = 0.001 mM (Table I, last column), are characteristic of correct incorporations occurring on misaligned DNA rather than misincorporations on properly aligned DNA (51).

α holoenzyme behaves differently from pol III holoenzyme in this respect. It does not appear to catalyze misalignment misincorporation. Misincorporation frequencies for dGMP·G and dTMP·G by α holoenzyme are the same on the two templates, and the K_m values are in the range of about 1.8 mM to >3 mM (Table I, data columns 2 and 3). Thus, despite the fact that both α and pol III core exhibit high processivity in the presence of the β sliding clamp, the two holoenzymes appear to differ significantly in their interactions at the primer-3′ terminus.

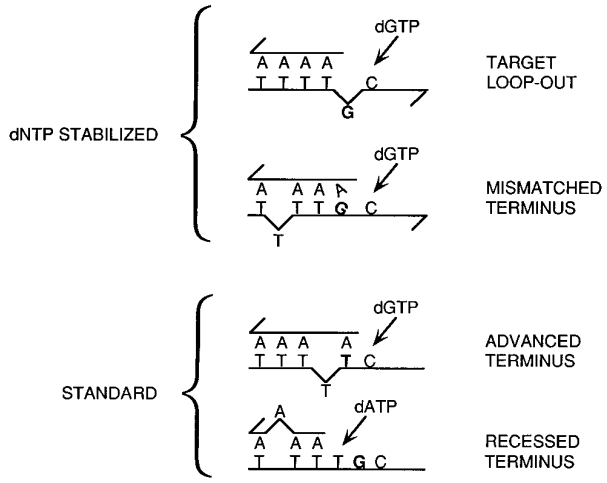

FIG. 8. **Possible misaligned primer/template DNA transient structures causing base substitution and frameshift mutations.** Standard misalignment model: structures are characterized by a properly annealed primer terminus which stabilizes a looped out base in the double-stranded region. When the target site (*boldface*) is complementary to the 3′-end of the primer, a template base can loop out and the primer terminus can advance to pair with the target site, presenting the downstream site (**T+1**) for the next insertion step (*ADVANCED TERMINUS*). This is not possible in our system because the target G is not complimentary to the primer terminal base, A. Alternately, when the **T−2** template base is complementary to the 3′-end of the primer, a primer base can loop out and the primer terminus can recede to pair with the **T−2** site, presenting the **T−1** site for the next insertion step (*RECESSED TERMINUS*). This is not observed in our system. dNTP-stabilized misalignment model: structures are characterized by an impediment at the primer terminus that might conventionally be expected to inhibit further extension. Target loop-out: insertion of rescue nucleotide opposite the **T+1** site is permitted when the target base loops out. This structure can occur in any sequence context. Mismatched terminus: A standard misalignment structure lacking a proper base pair at the primer terminus. This structure would take advantage of the particular sequence context used in our experiment. The A·G mispair at the primer terminus can be stabilized by two hydrogen bonds with the bases present as either anti·anti or anti·syn conformers (56–59).

Misalignment as a Possible Explanation for Reduced Fidelity in the Presence of Rescue Nucleotides—We suggest that elevated values of dGMP·G or dTMP·G occurring when pol III holoenzyme copies templates with C or A downstream from the target G, respectively, can be accounted for by a novel "dNTP-stabilized" primer/template misalignment. Misaligned p/t DNA structures have been proposed to account for slippage mispairing events leading to frameshift and base substitution mutations for normal (52–54) and damaged DNA (55). In the standard misalignment model (Fig. 8, advanced terminus), a primer terminus annealed to a complementary downstream template base is present to stabilize the misaligned p/t DNA. This misaligned structure is not possible on our templates, since the immediate downstream bases are not complementary to the primer terminus. Similarly, slippage within the run of four primer As (Fig. 8, recessed terminus) would cause a marked elevation in dAMP·G misincorporation. The observation that f_{inc} (dAMP·G) is very low (4.2×10^{-7}, Fig. 6*A, dATP lanes*) suggests that slippage of the primer strand does not occur.

Instead, we propose that the misaligned structure is stabilized by a dNTP substrate bound at the polymerase active site which is complementary to the template base downstream from the target site. We refer to this as the "dNTP-stabilized" misalignment model (Fig. 8). We have recently proposed that this novel type of misalignment may explain abasic lesion bypass catalyzed by human DNA polymerase β (34). In the present context, the model applies as follows: a dGMP is not inserted directly opposite the target G site, but is instead inserted

opposite a template C, immediately downstream from *G* (Fig. 8, target loop-out). This correctly inserted dGMP can then either be extended, resulting in a −1 frameshift error, or template realignment can occur, relocating dGMP opposite G and resulting in a base substitution (52–54). Such dNTP-stabilized misalignment is most likely to result in a frameshift mutation, but base substitutions can also occur (34).

Two different misaligned p/t DNA structures are possible (Fig. 8): (i) a loopout of the target G or (ii) displacement of any one of the four Ts, within the run of four consecutive A·T base pairs, and subsequent formation of a mispaired A·G terminus. NMR analysis has shown that A·G mispairs can be stabilized by two hydrogen bonds when either base is present in an *anti* or *syn* conformation (56–59). On the other hand, one might expect that the proofreading capacity of the pol III holoenzyme would be active on such an irregular primer-3′ terminus. We note that the target loop-out structure is independent of sequence context, whereas the mismatched terminus structure is sequence-dependent, which suggests an experimental design that might distinguish between the two.

Another possible explanation for the low pol III holoenzyme fidelity is inhibition of exonuclease activity. dGMP or dTMP might be misincorporated directly opposite the target G and primer slippage might then align the mismatched terminal nucleotide opposite the matched downstream template base via a standard misalignment mechanism (52–54). In this scenario, misalignment would occur after rather than before the misincorporation event and the misaligned structure might be sufficiently stable to inhibit proofreading.

Although, we cannot rule out this possibility, we favor the dNTP-stabilized misalignment model based on the extremely low K_m values observed. The K_m values (1 and 13 μM, Table I) accompanying the dTMP·G and dGMP·G misincorporation events are difficult to reconcile with nucleotide misincorporation on a properly aligned DNA molecule. These low K_m values are characteristic of correct incorporations rather than misincorporations (Table I). The K_m values characterizing direct misincorporations forming these same mispairs in a "nonslip" sequence context are about 1000-fold higher, 1.4 mM and >3 mM (Table I).

Application of the Gel Kinetic Assay to Measurement of High Fidelity—We have previously shown that the ratio of integrated gel band intensities, $I_{\mathbf{T}}^{\infty}/I_{\mathbf{T-1}}$, where **T** represents an arbitrary template target site, can be used to obtain the efficiency for misincorporation by a polymerase with exonuclease activity (Fig. 1, Equation 1), provided that the reaction conditions allow only single completed hits (SCH conditions) (20). SCH conditions mean that a polymerase extends a given p/t DNA molecule at most once, and then dissociates. As a corollary, the fraction of primer molecules extended multiple times must be negligible compared with those that are extended only once. The fractions of singly and multiply hit primers can easily be calculated from the fraction of unextended (unhit) primers using a Poisson distribution (20).

Reactions can usually be carried out under SCH conditions by using a large excess of either p/t DNA molecules or some other suitable trapping molecule, such as unlabeled DNA or heparin. However, this may not be the case for reactions measuring misincorporations, because low rates for the misincorporation reaction, typically 10^{-4}-10^{-7} compared with correct incorporation rates, may require that the enzyme encounter a p/t DNA multiple times to generate a detectable misincorporation band.

A general analysis for the evolution of primer extension bands under MCH conditions is given in the "Appendix" (60). Reactions both with and without exonuclease activity and with and without rescue nucleotides are considered. It is shown that without or with exonuclease, a simple correction factor relates the measured MCH V_{max}/K_m to the SCH V_{max}/K_m (Equations 20 and 22 in the "Appendix" (60)). The main result is that the correction factor can be very large when the incorporation rate is high (*e.g.* for the right nucleotide) and negligible when the incorporation rate is low (*e.g.* for the wrong nucleotide), see the "Appendix" (60).

The "bottom line" is that SCH conditions should always be used for measurements with the right nucleotide but, when MCH conditions are required to detect incorporation of a wrong nucleotide, then the correction factor calculated in the "Appendix" (60) (at most, a weighted sum of the number of hits) can be used to extract the SCH V_{max}/K_m for the misincorporated nucleotide (Equations 20 and 22). The analysis confirms the robust nature of the gel kinetic assay. Utilization of up to 80% of the primer under MCH conditions requires less than a 2-fold correction.

REFERENCES

1. Trautner, T. A., Swartz, M. N., and Kornberg, A. (1962) *Proc. Natl. Acad. Sci. U. S. A.* **48,** 449–455
2. Freese, E. (1959) *Proc. Natl. Acad. Sci. U. S. A.* **45,** 622–633
3. Freese, E. (1959) *J. Mol. Biol.* **1,** 87–105
4. Echols, H., and Goodman, M. F. (1991) *Annu. Rev. Biochem.* **60,** 477–511
5. Goodman, M. F., Creighton, S., Bloom, L. B., and Petruska, J. (1993) *Crit. Rev. Biochem. Mol. Biol.* **28,** 83–126
6. Nossal, N. G., and Alberts, B. M. (1983) in *Bacteriophage T4* (Mathews, C. K., Kutter, E. M., Mosig, G., and Berget, P. B., ed) pp. 71–81, American Society for Microbiology, Washington, D. C.
7. Nossal, N. G. (1994) in *Molecular Biology of Bacteriophage T4* (Karam, J. D., ed) pp. 43–53, American Society for Microbiology, Washington, D. C.
8. Maki, S., and Kornberg, A. (1988) *J. Biol. Chem.* **263,** 6561–6569
9. McHenry, C. S. (1988) *Annu. Rev. Biochem.* **57,** 519–550
10. Kelman, Z., and O'Donnell, M. (1995) *Annu. Rev. Biochem.* **64,** 171–200
11. Tabor, S., Huber, H. E., and Richardson, C. C. (1987) *J. Biol. Chem.* **262,** 16212–16223
12. Chalberg, M. D., and Kelly, T. J. (1989) *Annu. Rev. Biochem.* **58,** 671–717
13. Tsurimoto, T., and Stillman, B. (1991) *J. Biol. Chem.* **266,** 1950–1960
14. Stukenberg, P. T., Studwell-Vaughan, P. S., and O'Donnell, M. (1991) *J. Biol. Chem.* **266,** 11328–11334
15. Kong, X.-P., Onrust, R., O'Donnell, M., and Kuriyan, J. (1992) *Cell* **69,** 425–437
16. Fay, P. J., Johanson, K. O., McHenry, C. S., and Bambara, R. A. (1981) *J. Biol. Chem.* **256,** 976–983
17. Watanabe, S. M., and Goodman, M. F. (1978) *J. Virol.* **25,** 73–77
18. Kunkel, T. A., Patel, S. S., and Johnson, K. A. (1994) *Proc. Natl. Acad. Sci. U. S. A.* **91,** 6830–6834
19. Mozzherin, D. Ju., McConnell, M., Jasko, M. V., Krayevsky, A. A., Tan, C.-K., Downey, K. M., and Fisher, P. A. (1996) *J. Biol. Chem.* **271,** 31711–31717
20. Creighton, S., and Goodman, M. F. (1995) *J. Biol. Chem.* **270,** 4759–4774
21. Studwell, P. S., and O'Donnell, M. (1990) *J. Biol. Chem.* **265,** 1171–1178
22. Dong, Z., Onrust, R., Skangalis, M., and O'Donnell, M. (1993) *J. Biol. Chem.* **268,** 11758–11765
23. Xiao, H., Crombie, R., Dong, Z., Onrust, R., and O'Donnell, M. (1993) *J. Biol. Chem.* **268,** 11773–11778
24. Studwell-Vaughan, P. S., and O'Donnell, M. (1991) *J. Biol. Chem.* **266,** 19833–19841
25. Onrust, R., Finkelstein, J., Naktinis, V., Turner, J., Fang, L., and O'Donnell, M. (1995) *J. Biol. Chem.* **270,** 13348–13357
26. Boosalis, M. S., Petruska, J., and Goodman, M. F. (1987) *J. Biol. Chem.* **262,** 14689–14696
27. Creighton, S., Bloom, L. B., and Goodman, M. F. (1995) *Methods Enzymol.* **262,** 232–256
28. Randall, S. K., Eritja, R., Kaplan, B. E., Petruska, J., and Goodman, M. F. (1987) *J. Biol. Chem.* **262,** 6864–6870
29. Bloom, L. B., Turner, J., Kelman, Z., Beechem, J. M., O'Donnell, M., and Goodman, M. F. (1996) *J. Biol. Chem.* **271,** 30699–30708
30. Galas, D. J., and Branscomb, E. W. (1978) *J. Mol. Biol.* **88,** 653–687
31. Clayton, L. K., Goodman, M. F., Branscomb, E. W., and Galas, D. J. (1979) *J. Biol. Chem.* **254,** 1902–1912
32. Watanabe, S. M., and Goodman, M. F. (1982) *Proc. Natl. Acad. Sci. U. S. A.* **79,** 6429–6433
33. Fersht, A. R. (1979) *Proc. Natl. Acad. Sci. U. S. A.* **76,** 4946–4950
34. Efrati, E., Tocco, G., Eritja, R., Wilson, S. H., and Goodman, M. F. (1997) *J. Biol. Chem.* **272,** 2559–2569
35. Petruska, J., and Goodman, M. F. (1985) *J. Biol. Chem.* **260,** 7533–7539
36. Mendelman, L. V., Boosalis, M. S., Petruska, J., and Goodman, M. F. (1989) *J. Biol. Chem.* **264,** 14415–14423
37. Cai, H., Bloom, L. B., Eritja, R., and Goodman, M. F. (1993) *J. Biol. Chem.* **268,** 23567–23572
38. Yu, H., and Goodman, M. F. (1992) *J. Biol. Chem.* **267,** 10888–10896
39. O'Donnell, M. E. (1987) *J. Biol. Chem.* **262,** 16558–16565
40. Sloane, D. L., Goodman, M. F., and Echols, H. (1988) *Nucleic Acids Res.* **16,** 6465–6475
41. Mo, J.-Y., and Schaaper, R. M. (1996) *J. Biol. Chem.* **271,** 18947–18953

42. Fersht, A. R., and Knill-Jones, J. W. (1981) *Proc. Natl. Acad. Sci. U. S. A.* **78,** 4251–4255
43. Fersht, A. R., Knill-Jones, J. W., and Tsui, W. C. (1982) *J. Mol. Biol.* **156,** 37–51
44. Fersht, A. R., and Knill-Jones, J. W. (1983) *J. Mol. Biol.* **165,** 633–654
45. Fersht, A. R., and Knill-Jones, J. W. (1983) *J. Mol. Biol.* **165,** 669–682
46. Fersht, A. R. (1985) *Enzyme Structure and Mechanism*, 2nd Ed., p. 112, W. H. Freeman, and Co., New York
47. Brutlag, D., and Kornberg, A. (1972) *J. Biol. Chem.* **247,** 241–248
48. Muzyczka, N., Poland, R. L., and Bessman, M. J. (1972) *J. Biol. Chem.* **247,** 7116–7122
49. Bessman, M. J., Muzyczka, N., Goodman, M. F., and Schnaar, R. L. (1974) *J. Mol. Biol.* **88,** 409–421
50. Brenowitz, S., Kwack, S., Goodman, M. F., O'Donnell, M., and Echols, H. (1991) *J. Biol. Chem.* **266,** 7888–7892
51. Boosalis, M. S., Mosbaugh, D. W., Hamatake, R., Sugino, A., Kunkel, T. A., and Goodman, M. F. (1989) *J. Biol. Chem.* **264,** 11360–11366
52. Kunkel, T. A. (1986) *J. Biol. Chem.* **261(29),** 13581–13587
53. Kunkel, T. A., and Soni, A. (1988) *J. Biol. Chem.* **263,** 14784–14789
54. Ripley, L. S. (1990) *Annu. Rev. Genet.* **24,** 189–213
55. Shibutani, S., and Grollman, A. (1993) *J. Biol. Chem.* **268,** 11703–11710
56. Patel, D. J., Kozlowski, S. A., Ikuta, S., and Itakura, K. (1984) *Fed. Proc.* **43,** 2663–2670
57. Kan, L. S., Chandrasegaran, S., Pulford, S. M., and Miller, P. S. (1983) *Proc. Natl. Acad. Sci. U. S. A.* **80(14),** 4263–4265
58. Brown, T., Hunter, W. N., Kneale, G., and Kennard, O. (1986) *Proc. Natl. Acad. Sci. U. S. A.* **83,** 2402–2406
59. Brown, T., Leonard, G. A., Booth, E. D., and Chambers, J. (1989) *J. Mol. Biol.* **207,** 455–457
60. Fygenson, D. K., and Goodman, M. F. (1997) *J. Biol. Chem.* **272,** 27931–27935